Characterization of a novel *FLI1* mutation in a family with thrombocytopenia and other congenital malformations

Inherited thrombocytopenias are a heterogeneous group of rare diseases, characterized by low platelet count, caused by mutations in at least 45 genes.

Among them, *FLI1* encodes a member of the E26 transformation-specific (ETS) family of transcription factors, which is characterized by a PNT domain for protein-protein interaction,[1] and an ETS domain involved in DNA binding at the consensus GGA(A/T) core motif.[2] *FLI1* is highly expressed during megakaryopoiesis, where it transcriptionally regulates many lineage-specific genes involved in megakaryocyte development and platelet biogenesis,[3] including *ITGA2B, GP1BA, GP6, GP9* and *MPL*.[4]

Haploinsufficiency of *FLI1* is the cause of the platelet defects in the Jacobsen syndrome (JBS, MIM 147791), a contiguous gene deletion syndrome due to the terminal deletion of 11q23-qter characterized by thrombocytopenia and excessive bleeding associated with a series of congenital malformations, including physical growth delay, psychomotor retardation, cardiac malformations, and facial dysmorphisms.[5] Platelets of JBS patients usually present defective function and are characterized by large fused α granules and δ granule deficiency.

The same hematological picture has been reported also in a few families affected by "platelet-type bleeding disorder-21" (BDPLT21, MIM 617443), also known as "*FLI1*-related thrombocytopenia" (FLI1-RT), caused by heterozygous or homozygous mutations in *FLI1*.

Here, we report a family with mild thrombocytopenia associated with additional congenital abnormalities (Table 1; Figure 1A). According to the Declaration of Helsinki, patients signed written informed consent.

The proband (III-1), born by cesarean section at 37 weeks of gestation following a physiological pregnancy (no reported teratogenic risks for drugs or infections during pregnancy), presented at birth with a reduction defect of the right upper limb consisting in slight reduction in the length of the homer, severe hypoplasia of the forearm, radius and ulna, absence of hand with presence of only cutaneous small sketches of the fingers (Figure 1B) and a large sub-aortic ventricular sept defect associated with medium-grade cardiomegaly, which was surgically corrected at 3 months of life. Ocular fundus examination, auditory brainstem response, abdominal ultrasound, and spine x-rays were normal. Psychomotor development was normal. At the age of 21, she experienced the onset of simple partial sensory-motor epileptic seizures. Electroencephalogram showed asynchronous bilateral epileptiform abnormalities in the right parietal and left temporal regions, while cerebral magnetic resonance imaging demonstrated right insular heterotopia and polymicrogyria, with periventricular

Table 1. Main clinical and laboratory features of the investigated subjects carrying the c.827delC variant of the *FLI1* gene.

Subject	Sex/age, years	Platelet count, x10⁹/L	MPV,[1] fL	Mean platelet diameter,[2] µM	Platelet diameter distribution width,[3] µM	ISTH BAT score[4]	Bleeding symptoms	Additional clinical findings
III-1	F/29	85-118	15.3	3.71	5.10	8	Easy bruising, menorrhagia	Reduction defects of the right upper limb, especially severe hypoplasia of the forearm and aplasia of the hand; severe ventricular sept defect with cardiomegaly; pachygyria, polymicrogyria, periventricular heterotopia, and seizures; patellar dislocation
II-2	F/52	77-132	14.7	3.52	5.02	25	Easy bruising, menorrhagia, epistaxis, gum bleeding	Patent forame ovale; mitral valve prolapse; bilateral camptodactyly of the II and V finger

[1]Mean platelet volume (MPV) evaluated by automated cell counter, reference values 8-13 fL. [2]Mean platelet diameter was assessed on peripheral blood smears through software-assisted image analysis, as previously reported.[14] Reference value obtained in 55 investigated healthy volunteers is 2.58 µm, with 95% confidence interval (CI): 2.4-2.7. [3]Platelet diameter distribution width assessed as previously reported.[14] Reference value obtained in in 55 healthy subjects is 2.3 µm, with 95% CI: 2.2-2.5. [4]International Society on Thrombosis and Hemostasis (ISTH) Bleeding Assessment Tool (BAT) score was assessed as previously reported.[15]

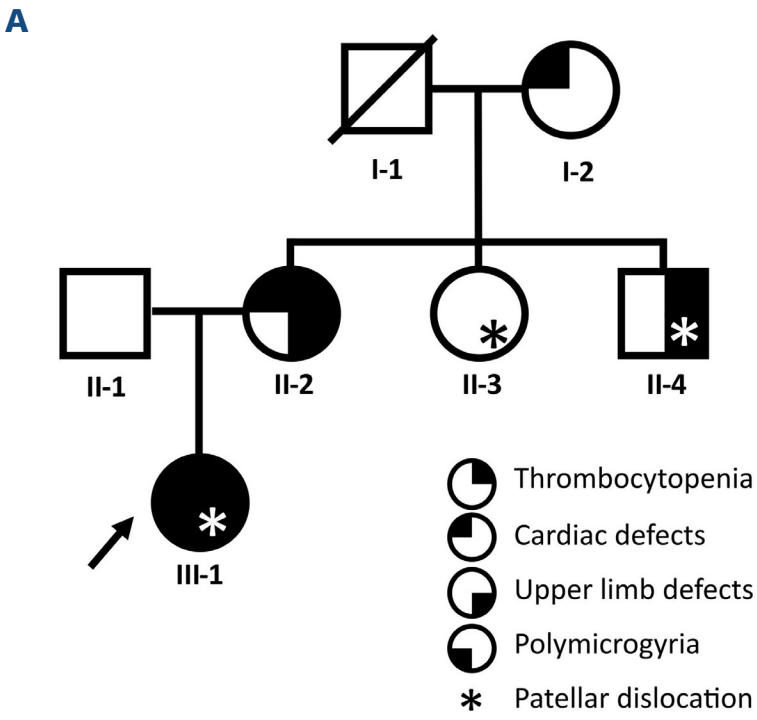

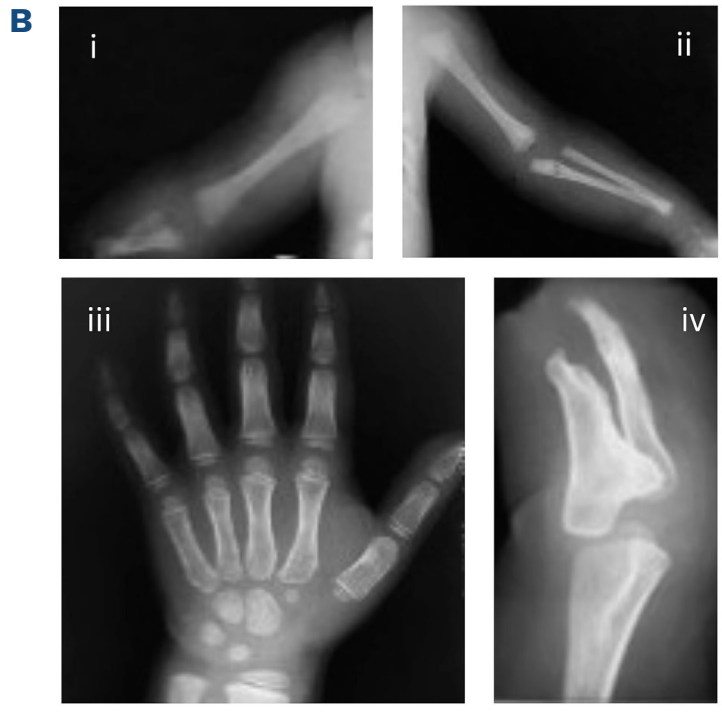

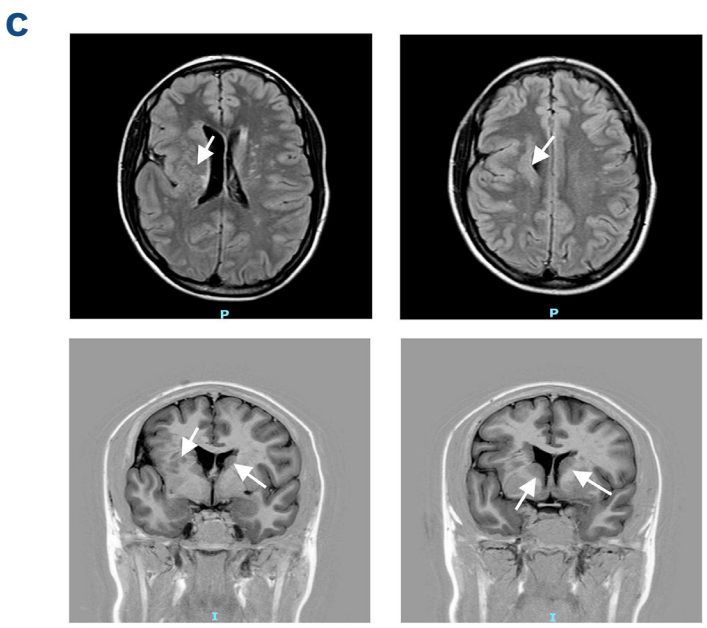

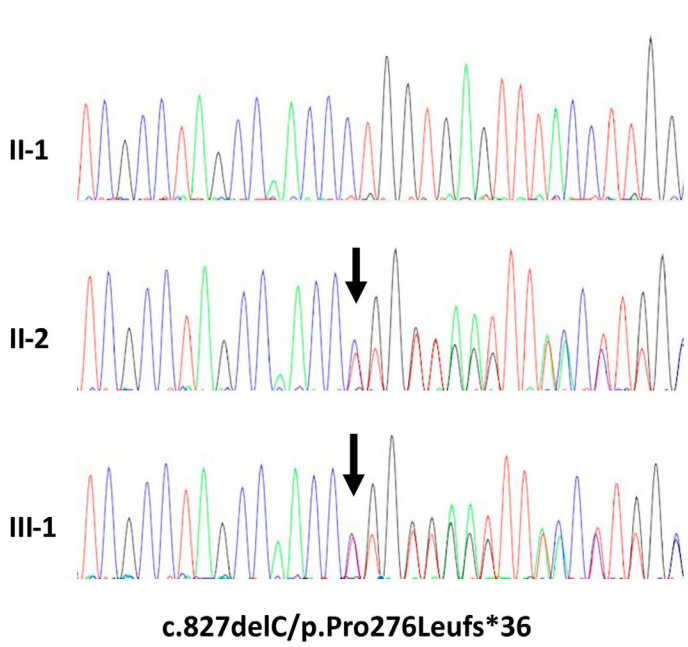

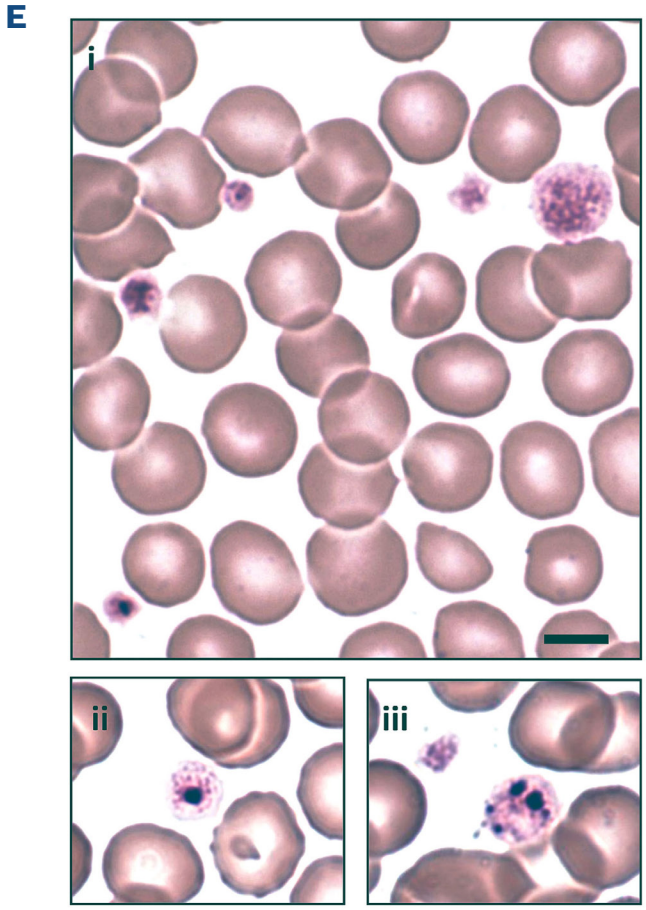

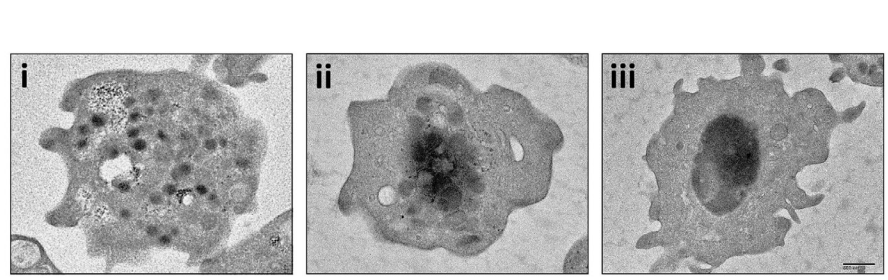

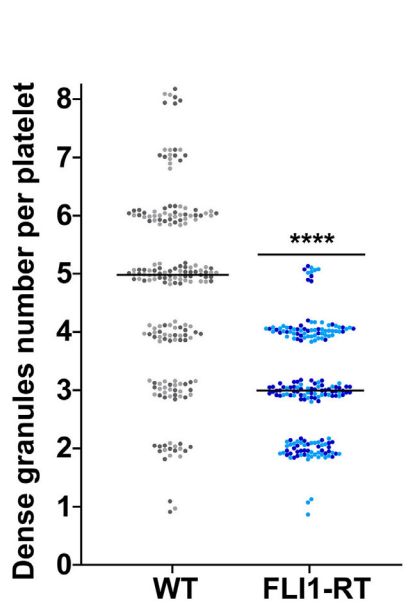

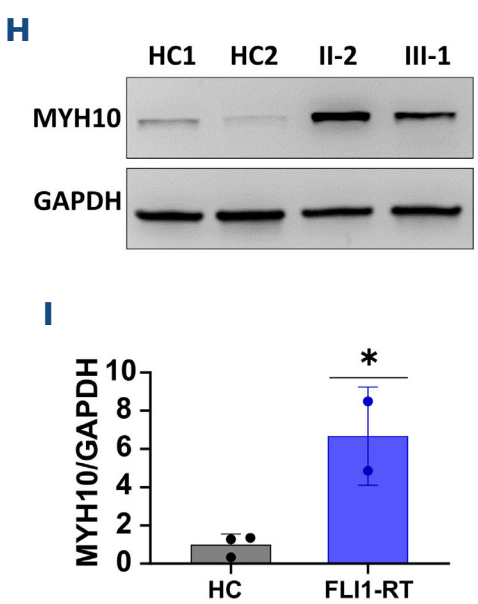

Continued on following page.

Figure 1. Phenotype and genotype description of a family affected by thrombocytopenia associated with extra-hematological features. (A) Clinical features of each family member are indicated in the pedigree. Black arrow indicates the proband (III-1). (B) Proband's upper limbs X-rays in the first days of life (i=right; ii=left) and at 4 years of age (iii=left; iv=right). Congenital malformations of the right upper limb with agenesis of the forearm (middle-distal third) and hand; presence of right radius and ulna proximal stumps, which appear thinned and with sinuous profiles at the distal end. The bones of the left hand are within the normal limits for age. (C) T2- FLAIR and T1-inversion recovery weighted brain magnetic resonance imaging (MRI) images with heterotopia and polymicrogyria in right insula and in left frontal horn (white arrows). (D) Electropherogram of Sanger sequencing in the proband and her parents performed to confirm the presence of the *FLI1* variant identified by whole-exome sequencing (WES). Individuals I-1, I-2, II-3 and II-4 were not available for segregation analysis. Arrows indicate c.827delC. (E) May-Grünwald-Giemsa stained blood smears of the proband (i, ii) and her mother (iii) showing platelet macrocytosis and anisocytosis, along with the evidence of large α granules or a single giant α granule. At least 200 platelets for each patient were investigated. Scale bars correspond to 5 μm. (F) Representative images of transmission electron microscopy (TEM) on patients' platelet sections. About 10% of platelets from both patients showed large confluent α granules (ii) or a single giant α granule (iii). A platelet with normal diffuse distribution of α granules is shown in (i) for comparison. (G) Δ granule content of II-1 (light blue) and II-2 (dark blue) patients carrying the c.827delC variant of *FLI1* (FLI1-RT), compared to 2 different healthy controls (HC) (HC1 in light grey and HC2 in dark grey). Jittered dots on the plot represent δ granule number per platelet measured by image analysis of TEM platelet sections. At least 100 platelets were analyzed for each individual. Lines represent the median. Differences were evaluated by analyses of variance (ANOVA) ****P<0.0001. (H) Representative image of MYH10 (3404S, Cell Signaling) immunoblotting of platelet lysates from patients (II-2 and III-1) or 2 different HC (HC1 and HC2). GAPDH (ab181602, Abcam) was used as loading control. (I) Densitometric analysis of immunoblots described in (H). Histogram bars represent MYH10/GAPDH mean ratio obtained for patient's platelets (FLI1-RT, blue bar) and 3 HC (grey bar). The actual points, shown as dots in the graph, represent the mean of the 3 values measured for each subject. Error bars represent standard deviation. *P<0.05, as determined by Student's *t* test. WT: wild-type.

heterotopic aspects also on the left side that extended to the region of the frontal horn (Figure 1C).

The proband also presented a lifelong history of mild thrombocytopenia with platelet count ranging between 85 and 118x10^9/L and increased mean platelet volume (MPV). She reported easy bruising and menorrhagia, which, on some occasions, required access to the emergency room (Table 1). The proband's 52-year-old mother (II-2) also had chronic macrothrombocytopenia (platelet count ranging between 77 and 132x10^9/L). She reported a lifelong history of bleeding manifestations, including easy bruising, menorrhagia, recurrent epistaxis, and gum bleeding. Furthermore, the proband's mother reported patent foramen ovale, mitral valve prolapse, and bilateral camptodactyly of the II and V fingers (Table 1). Of note, the association of chronic thrombocytopenia, radial hypoplasia, bilateral proximal radioulnar synostosis, and recurrent patellar dislocations, was reported in a proband's maternal uncle (II-4), who was not available for investigations.

After exclusion of JBS and thrombocytopenia-absent radius (TAR, MIM 274000)[6] by karyotype and CGH array analysis, as well as of Holt Oram syndrome (HOS, MIM 142900) by mutational screening of the *TBX5* gene,[7] whole-exome sequencing (WES) was performed in the proband and her parents to explain the complex syndromic phenotypes observed in the family. Trio WES analysis, extended to the Human Phenotype Ontology (HPO) genes associated with the patients' phenotypes (HP:0006496; HP:0001873; HP:0001629; HP:0002126; HP:0002282 and HP:0007359), did not identify any pathogenic or likely pathogenic variant, except for a novel heterozygous single nucleotide deletion (c.827delC) in the *FLI1* gene in the proband (III-1) and her mother (II-2) (Figure 1D).

This variant, affecting a highly evolutionarily conserved residue (*Online Supplementary Figure S1A*), is predicted to result in a frameshift truncated protein (p.P276Lfs36*) of approximately 34 kDa lacking the entire ETS domain, the DNA binding domain affected by the other known mutations of FLI1-RT[8-10] (*Online Supplementary Figure S1B*). Despite the complete disruption of the ETS domain, the AlphaFold2 model of p.P276Lfs36* predicts that its PNT domain retains the same conformational structure as that of the wild-type (WT) protein and thus probably its protein-protein interaction role (*Online Supplementary Figure S1C*).

Consistent with a mutation in *FLI1*, investigation of blood smears of the proband (III-1) and her mother (II-2) revealed platelet macrocytosis and anisocytosis, with 7% to 10% of platelets presenting one or more giant α granules,[10] a typical finding of FLI1-RT that was confirmed by transmission electron microscopy analysis (Figure 1E, F; Table 1) and immunofluorescence staining with the α granule marker thrombospondin-1 (*Online Supplementary Figure S2A*). Moreover, patients' platelets showed a moderate reduction in the δ granule content (Figure 1G; *Online Supplementary Figure S2B*). *In vitro* platelet function could not be investigated as patients' fresh blood sample were not available. However, for both patients, bleeding history was much more severe than expected based on their mild thrombocytopenia (Table 1), supporting an associated platelet dysfunction. Finally, since aberrant expression of the MYH10 protein in platelets is a biomarker for pathogenic variants in the *FLI1, RUNX1* or *GATA1* transcription factor genes,[8-12] we performed immunoblotting analysis of platelets from III-1 and II-2, which showed a clear expression of MYH10 (Figure 1H, I), further supporting the pathogenic role of the c.827delC variant and the diagnosis of FLI1-RT.

Hypothesizing a reduction in FLI1 protein expression due to the frameshift mutation, we analyzed FLI1 protein in the patients' platelets by immunoblotting. We observed a reduction of the WT-FLI1 protein of 51 KDa (p51) compared to healthy controls, as expected, and another highly expressed product of approximately 34 KDa (p34). In addition to matching the

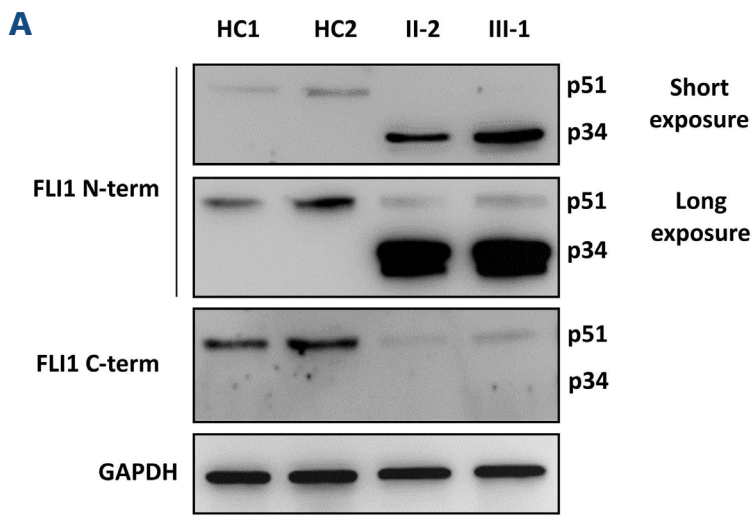

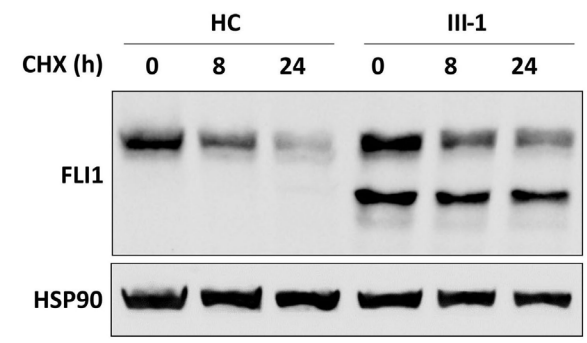

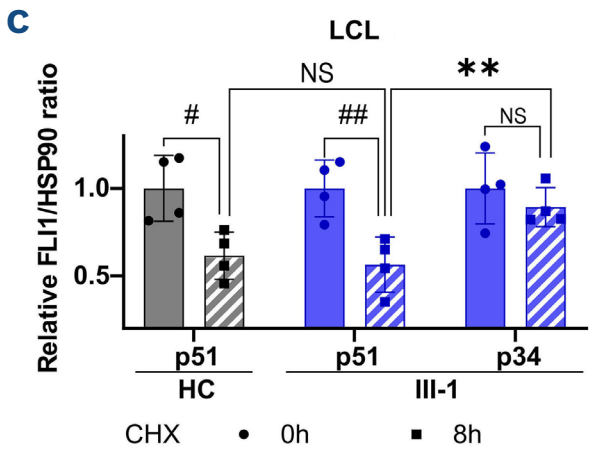

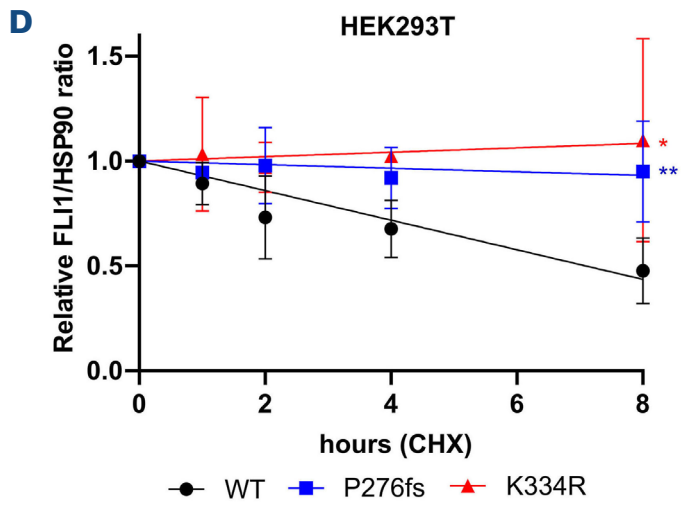

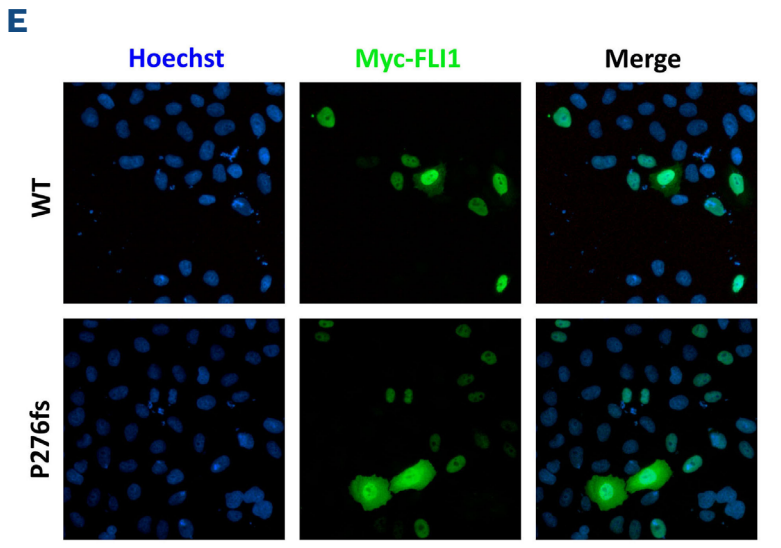

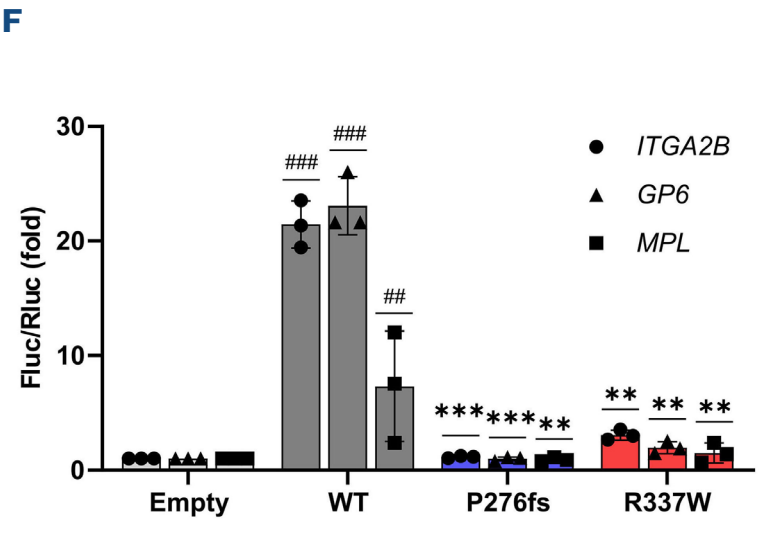

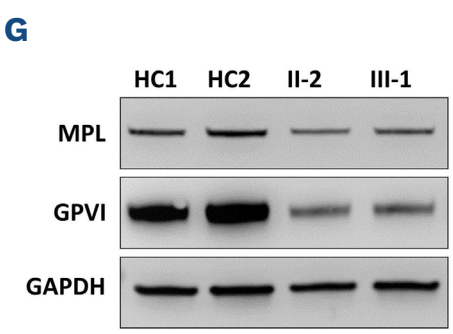

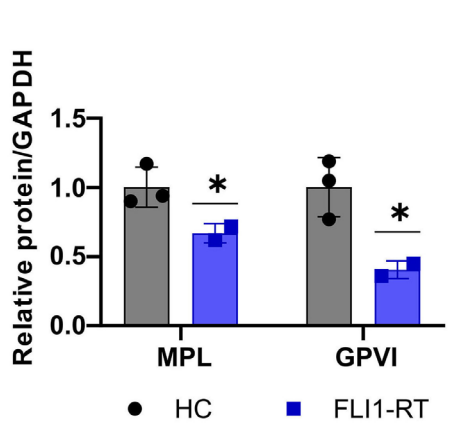

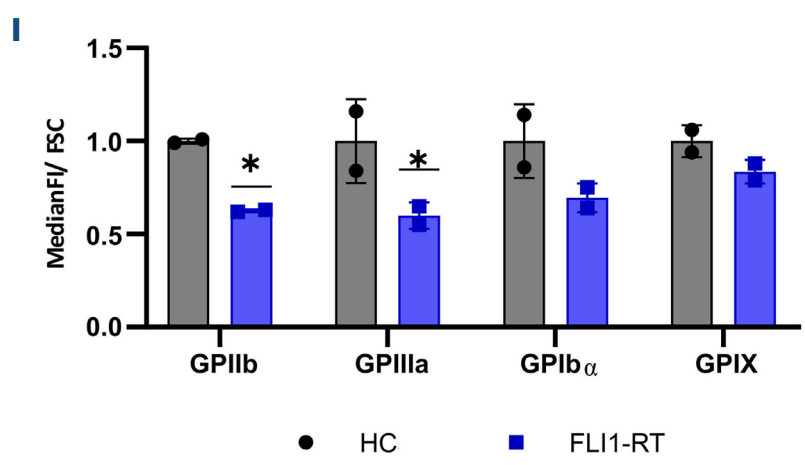

Figure 2. Pathogenetic nature and increased stability of p.P276Lfs36* mutant protein. (A) Immunoblotting analysis of platelets lysates from patients (II-2 and III-1) or 2 different healthy controls (HC) (HC1 and HC2) using antibodies recognizing the N-terminus (ab124791, Abcam) and C-terminus (ab180902, Abcam) of FLI1. p51 and p34 indicate the wild-type (WT) FLI1 protein and the p.P276Lfs36* mutant product, respectively. GAPDH (ab181602, Abcam) was used as loading control. (B) Immunoblotting of lym-

Continued on following page.

phoblastoid cell lines protein samples from control (HC) and patient III-1 treated with cycloheximide (CHX, C4859, Sigma-Aldrich) 50 µg/mL and collected at different time points (0, 8 and 24 hours [h]). HSP90 (sc-13119, Santa Cruz) was used as loading control. (C) Histogram represents the densitometric analysis of 4 independent immunoblots described in (B). Striped bars indicate the relative mean FLI1/HSP90 ratio after 8 h of treatment, normalized on time 0 h (full bars). In III-1 LCL (blue bars), semi-quantitative analyses were performed independently for p51 and p34. HC ratios reported as grey bars. Dots/squares indicate the actual data. Error bars represent standard deviation (SD). Error bars represent SD. Student's *t* test was performed to assess the statistical relevance of reduction of the different forms of FLI1 after CHX treatment ($^{\#}P<0.05$; $^{\#\#}P<0.01$) or between different forms at 8 h of treatment both in the patient and healthy control ($^{**}P<0.01$); NS: not significant. (D) Semi-quantitative analysis of immunoblotting assay of HEK293T cells lysates after overexpression of WT, P276Lfs36*, or K334R forms of FLI1 treated with 50 µg/mL CHX and collected at different time points (0, 2, 4 and 8 h). Graph points indicate the mean of the relative FLI1/HSP90 ratio compared to time 0 h. The different forms of FLI1 are reported with black dots (WT), red triangles (P276Lfs36*), and blue squares (K334R). Error bars represent SD of at least 3 independent experiments. Student's *t* test was performed to demonstrate the different stability of P276Lfs36* and K334R with respect to WT at the 8-h time point. $^{*}P<0.05$ and $^{**}P<0.01$. (E) WT and P276Lfs36* FLI1 (green) transfected in HeLa cells were detected by anti-Myc antibody (sc-40, Santa Cruz) in immunofluorescence assays. Nuclei were labeled with Hoechst stain (blue). (F) Gene reporter assays performed in HEK293T cells overexpressing the WT (grey), P276Lfs36* (blue), or R337Q (used as control, red) forms of *FLI1*, cloned in pCDNA3.1 vector. Cells were co-transfected with the pGL4 reporter constructs expressing the firefly (*P. pyralis*) luciferase gene under the control of the *ITGA2B* (dots), *GP6* (triangles) or *MPL* (squares) promoter and the pRL *Renilla* luciferase control reporter vector. Histograms show the mean of firefly/renilla luciferase ratio normalized on that of cells transfected with the pCDNA3.1 empty vector sample. Error bars represent SD of 3 independent experiments. $^{\#\#}P<0.01$ and $^{\#\#\#}P<0.001$ are *versus* empty vector. $^{**}P<0.01$, and $^{***}P<0.001$ are *versus WT-FLI1* overexpression, as determined by Student's *t* test. (G) Representative image of GPVI (ab129019, Abcam) and MPL (ab109003, Abcam) immunoblotting on platelet lysates from II-2 and III-1 or 2 different HC (HC1 and HC2). GAPDH (ab181602, Abcam) was used as loading control. (H) Densitometric analysis immunoblotting described in (G). Histogram bars indicate the relative protein/GAPDH mean ratio of patients (FLI1-RT, grey bars, dots) or HC platelets (blue bars, squares). The actual points, shown as dots in the graph, represent the mean of the 3 values measured for each subject. Error bars represent standard deviation. $^{*}P<0.05$, as determined by Student's *t* test. (I) Histogram represents the expression of the subunits (GPIIb and GPIIIa) of the GPIIb-IIIa complex or the subunits (GPIbα and GPIX) of the GPI-IX complex assessed through flow cytometry assay on FLI1 patients' platelets (FLI1-RT, blue bars, squares) compared to HC (grey bars, dots), assessed in parallel. CD41 (IM0649U, Beckman Coulter) and CD61 (61F-100T, Immunostep) antibodies were used to detect GPIIb and GPIIIa subunits, respectively. CD42A (IM1757U, Beckman Coulter) and CD42B (IM0648U, Beckman Coulter) were used to detect GPIX and GPIBα subunit, respectively. Expression of the glycoproteins was calculated as the ratio between the median fluorescence intensity and platelet size (FSC: forward scatter channel). Data are presented as the means ± SD relative to control samples assessed in parallel, set as 1; $^{*}P<0.05$ as determined by Student's *t* test.

expected molecular weight of the c.827delC protein product, the p34 band was detectable with an antibody specific for the N-terminus of FLI1, but not with an antibody against the C-terminus, further suggesting that it actually corresponds to the truncated p.P276Lfs36* (Figure 2A).

The high expression level of p34 detected even in the Epstein-Barr virus immortalized lymphoblastoid cell line (LCL) established from the proband (III-1) (*Online Supplementary Figure S3A*), led us to investigate its half-life. A significant decrease of p51 was observed in both III-1 and healthy control LCL after 8 and, more remarkable, after 24 hours (h) of treatment with cycloheximide (CHX), while the p34 protein was significantly more stable (Figure 2B, C). Since polyubiquitination of lysine at position 334 (K334) is important for the proper turnover of FLI1,[13] we speculated that the high expression level of p.P276Lfs36* is due to the lack of this critical residue, which prevents the mutant protein from being degraded by the ubiquitin-proteasome system.

To verify this hypothesis, we treated HEK293T cells overexpressing the WT or p.P276Lfs36* cDNA of FLI1, as well as the non-ubiquitinable mutant p.K334R,[13] with CHX. Immunoblotting analysis confirmed that, after 8 h of treatment, the levels of p.P276Lfs36* and p.K334R were only slightly decreased with respect to untreated cells (CHX, 0 h), in contrast to the WT protein, which reached its half-life at the same time point (Figure 2D; *Online Supplementary Figure S3B*). This suggests that the high expression of the p.P276Lfs36* protein observed in patients' samples is due to its increased stability.

Immunofluorescence assays in HeLa cells showed that p.P276Lfs36* FLI1 is mainly localized in the nuclear compartment similarly to the WT-FLI1 (Figure 2E), but in contrast with other investigated FLI1 pathogenic variants (p.R337Q and p.K345E), which accumulate in the cytoplasm.[10] Finally, gene reporter assay performed in HEK293T cells demonstrated that p.P276Lfs36* does not exert any transcriptional activity on the promoters of some of the known FLI1 target genes (*MPL, GP6* and *ITGA2B*),[4] as well as p.R337W used as control[8] (Figure 2F).

Overall, these findings indicate that, despite its high expression and preserved ability to translocate to the nucleus, p.P276Lfs36* FLI1 does not exert its canonical transcriptional activities, in keeping with the complete loss of its ETS domain. Accordingly, we observed a strongly impaired expression of the collagen receptor glycoprotein GPVI and a moderate reduction of the thrombopoietin receptor MPL in patients' platelet lysates (Figures 2G, H). Moreover, consistent with a defective transactivation of *ITGA2B*, the gene encoding the GPIIb glycoprotein, flow cytometry revealed a reduced expression of the GPIIb-IIIa glycoprotein complex on platelet membrane in both affected individuals. Expression of the GPIb-IX complex subunits, encoded by *GP1BA* and *GP9*, was also decreased, although to a lesser extent than GPIIb-IIIa (Figure 2I).

In conclusion, the novel (c.827delC) pathogenic variant identified in the family explains the thrombocytopenia typical

of FLI1-RT. The family members are also affected by other congenital phenotypes that have not been reported in the other few FLI1-RT patients.[8-10] Although the genetic causes of these extra-hematological manifestations are likely to be explained by variants not detected by WES, we cannot exclude that the abundance and nuclear localization of p.P276Lfs36*, which loses DNA-binding activity but probably maintains the protein-protein interaction through an intact PNT domain, may allow the mutant protein to exert unknown non-canonical functions that could contribute, at least in part, to these phenotypes.

Authors

Daniele Ammeti,[1*] Serena Barozzi,[2*] Alessandro Pecci,[2,3] Melania Eva Zanchetta,[1] Edward Cesnik,[4] Alessandra Ferlini,[5,6] Mariabeatrice Sanchini,[5,6] Laura Verga,[7] Valeria Bozzi,[2] Fabio Corsolini,[8] Michela Faleschini,[1] Anna Savoia[9] and Stefania Bigoni[5,6]

[1]Institute for Maternal and Child Health, IRCCS Burlo Garofolo, Trieste; [2]Medical Department, IRCCS Policlinico San Matteo Foundation, Pavia; [3]Department of Internal Medicine, University of Pavia, Pavia; [4]Neurology Unit, Ferrara University Hospital, Ferrara; [5]Medical Genetics Unit, Department of Mother and Child, Ferrara University Hospital and University of Ferrara, Ferrara; [6]Department of Medical Sciences, Ferrara University Hospital and University of Ferrara, Ferrara; [7]Pathology Unit, Department of Molecular Medicine, IRCCS Policlinico San Matteo Foundation, Pavia; [8]Hematology Unit, IRCCS Istituto Giannina Gaslini, Genoa and [9]Department of Engineering for Innovation Medicine, University of Verona, Verona, Italy

*DA and SB contributed equally as first authors.

Correspondence:
M. FALESCHINI - michela.faleschini@burlo.trieste.it
A. SAVOIA - anna.savoia@univr.it

https://doi.org/10.3324/haematol.2024.287120

Received: December 23, 2024.
Accepted: May 26, 2025.
Early view: June 5, 2025.

Disclosures

No conflicts of interest to disclose.

Contributions

MF, AS and SBi designed the study. DA performed genetic analyses and *in vitro* functional assays. SBa and VB performed platelet studies. MEZ performed stability assays. LV performed TEM analysis. FC generated lymphoblastoid cell lines. EC, AF, MS and SBi enrolled patients and collected clinical data. DA, SBa, AP, MF, AS and SBi interpreted data. DA, AP, MF, MS and AS wrote the manuscript. SBa, AF and SBi critically reviewed the manuscript. All authors read and approved the manuscript.

Funding

This study was funded by the Italian Ministry of Health, through the contribution given to the Institute for Maternal and Child Health IRCCS Burlo Garofolo, Trieste, Italy (grant number: RC28/22 and RC02/23) and through the contribution given to IRCCS Policlinico San Matteo Foundation, Pavia, Italy (GR-2018-12367235 and RC-2019–08068819). Ferrara University Hospital is a member of the European Reference Network on Rare Congenital Malformations and Rare Intellectual Disability ERN-ITHACA [EU Framework Partnership Agreement ID: 3HP-HP-FPAERN-01-2016/739516].

Data-sharing statement

All data relevant to the study, together with the Materials and Methods details not included in the manuscript, are available upon request to the corresponding author.

References

1. Kwiatkowskit BA, Bastian LS, Bauer TR, Tsai S, Zielinska-Kwiatkowska AG, Hickstein DD. The ets family member tel binds to the Fli-1 oncoprotein and inhibits its transcriptional activity. J Biol Chem. 1998;273(28):17525-17530.
2. Oikawa T, Yamada T. Molecular biology of the Ets family of transcription factors. Gene. 2003;303:11-34.
3. Li Y, Luo H, Liu Z, Zacksenhaus E, Ben-David Y. The ets transcription factor Fli-1 in development, cancer and disease. Oncogene. 2014;34(16):2022-2031.
4. Songdej N, Rao AK. Hematopoietic transcription factor mutations: Important players in inherited platelet defects. Blood. 2017;129(21):2873-2881.
5. Mattina T, Perrotta CS, Grossfeld P. Jacobsen syndrome. Orphanet J Rare Dis. 2009;4:9.
6. Toriello HV. Thrombocytopenia-absent radius syndrome. Semin Thromb. 2011;37(6):707-712.
7. Vanlerberghe C, Jourdain A-S, Ghoumid J, et al. Holt-Oram syndrome: clinical and molecular description of 78 patients with TBX5 variants. Eur J Hum Genet. 2019;27(3):360-368.
8. Stockley J, Morgan NV, Benet D, et al. Enrichment of FLI1 and RUNX1 mutations in families with excessive bleeding and platelet dense granule secretion defects. Blood. 2013;122(25):4090-4093.
9. Stevenson WS, Rabbolini DJ, Beutler L, et al. Paris-Trousseau thrombocytopenia is phenocopied by the autosomal recessive inheritance of a DNA-binding domain mutation in FLI1. Blood. 2015;126(17):2027-2030.
10. Saultier P, Vidal L, Canault M, et al. Macrothrombocytopenia and dense granule deficiency associated with FLI1 variants: ultrastructural and pathogenic features. Haematologica.

2017;102(6):1006-1016.
11. Antony-Debré I, Bluteau D, Itzykson R, et al. MYH10 protein expression in platelets as a biomarker of RUNX1 and FLI1 alterations. Blood. 2012;120(13):2719-2722.
12. Machlus KR, Italiano JE Jr. The incredible journey: from megakaryocyte development to platelet formation. J Cell Biol. 2013;201(6):785-796.
13. Gierisch ME, Pfistner F, Lopez-Griec LA, Harder L, Schäfer BW, Niggli FK. Proteasomal degradation of the EWS-FLI1 fusion protein is regulated by a single lysine residue. J Biol Chem. 2016;291(52):26922-26933.
14. Noris P, Biino G, Pecci A, et al. Platelet diameters in inherited thrombocytopenias: analysis of 376 patients with all known disorders. Blood. 2014;124(6):e4-e10.
15. Gresele P, Orsini S, Noris P, et al. Validation of the ISTH/SSC bleeding assessment tool for inherited platelet disorders: a communication from the Platelet Physiology SSC. J Thromb Haemost. 2020;18(3):732-739.